

# Effect of nickel content on the formation and properties of amorphous $\text{Al}_{100-x}\text{RE}_5\text{Ni}_x$ alloys

W. S. SUN, M. X. QUAN, S. L. LI

*Laboratory of Rapidly Solidified Non-Equilibrium Alloys, Institute of Metal Research, The Chinese Academy of Sciences, Shenyang 110015, People's Republic of China*

The thermal stability and formation range of amorphous  $\text{Al}_{100-x}\text{Ln}_5\text{Ni}_x$  ( $x = 3, 5, 9, 13, 17, 21, 23$ ) alloys were studied by differential scanning calorimetry and X-ray diffraction techniques. The microhardness,  $H_v$ , of these Al–RE–Ni alloys was measured. The experimental results show that toughness was adversely affected by increase in the nickel content. The atomic size factor was applied to explain the formation mechanism of aluminium-based amorphous alloys by the atomic clusters model. The minimum concentration of nickel in Al–RE–Ni alloys results from the effective atomic volume difference of the nickel and aluminium atoms.

## 1. Introduction

It is known that the amorphization of metallic materials causes remarkable increases in mechanical properties [1, 2]. Using the rapid solidification technique from the melt, a large range of metastable microstructure can be achieved, providing a large variety of physical properties, particularly in the mechanical areas. On the other hand, when the alloys are amorphous, heat treatment also leads to structural modification which is of great concern in every application [3, 4]. Ternary compounds have a great advantage in that they can give rise to physical properties not present in binary alloys [5]. In aluminium-based amorphous alloys the ternary compound is composed of rare-earths and transition metals, which are alloyed to produce a better formation ability for the amorphization of the melt. The high mechanical strength and good ductility of amorphous alloys in the Al–Ln–TM system [6] have recently been clarified.

In the present work, studies on the thermal and mechanical properties of amorphous  $\text{Al}_{100-x}\text{RE}_5\text{Ni}_x$  alloys were carried out. The formation range was examined by X-ray diffraction (XRD) and differential scanning calorimetry (DSC) techniques. The experimental results were compared with the previous theory, which predicts the minimum solute concentration necessary to form a stable glass. The effects of nickel content on the toughness and microhardness are reported.

## 2. Experimental procedure

The ingot was prepared by induction melting the mixture of pure metals. The ternary alloys with composition  $\text{Al}_{100-x}\text{RE}_5\text{Ni}_x$  were used in the present alloys ( $x = 3, 5, 9, 13, 17, 21, 23$ ), where RE is a mixture of rare-earth metals composed of  $\text{La}_{10}\text{Ce}_5\text{Pr}_{15}\text{Nd}_{10}$ . The composition is normally expressed in atomic per

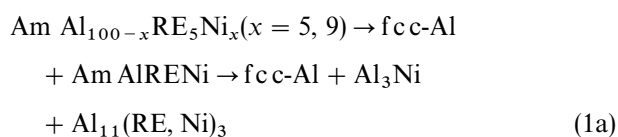
cent. The amorphous ribbons were prepared by the melt-spinning technique with a linear velocity of  $35 \text{ ms}^{-1}$  in an argon atmosphere. The amorphous and crystalline phases were checked by  $\text{CuK}_\alpha$  ( $\lambda = 0.15405 \text{ nm}$ ) X-ray diffractometry. For  $x = 3, 23$ , the structures were amorphous + crystalline phase. For  $x = 5, 9, 13, 17, 21$ , the structures were all in the amorphous state (Fig. 1a). The thermal properties were measured by DSC (Perkin–Elmer DSC-7) at a heating rate  $20 \text{ K min}^{-1}$ . The microhardness was measured using a 15 g load on Vickers hardness tester; the tensile fractographs were observed by scanning electron microscopy (SEM).

## 3. Results and discussion

### 3.1. The thermal stability of amorphous $\text{Al}_{100-x}\text{RE}_5\text{Ni}_x$ alloys

Typical DSC scanning records are shown in Fig. 2 for amorphous  $\text{Al}_{100-x}\text{RE}_5\text{Ni}_x$  alloys at a constant heating rate of  $20 \text{ K min}^{-1}$ . Table I shows the thermal parameters of amorphous  $\text{Al}_{100-x}\text{RE}_5\text{Ni}_x$  alloys. For  $x = 5, 9$ , two exothermic peaks were evident in the DSC curves. Only one exothermic peak was found when  $x = 13, 17, 21$ .

The amorphous alloys  $\text{Al}_{90}\text{RE}_5\text{Ni}_5$  and  $\text{Al}_{86}\text{RE}_5\text{Ni}_9$  were annealed at 453 K for 1 h. Nanoscale fcc-Al was discovered in an amorphous matrix. The average grain sizes were found to be 11 and 19 nm by Stock's method from the Scherrer formula (see Fig. 1b). The crystallization products were fcc-Al and intermetallic compounds  $\text{Al}_3\text{Ni}$  and  $\text{Al}_{11}(\text{RE}, \text{Ni})_3$  when they were annealed at 613 K for 1 h (see Fig. 1c). So the crystallization process can be written



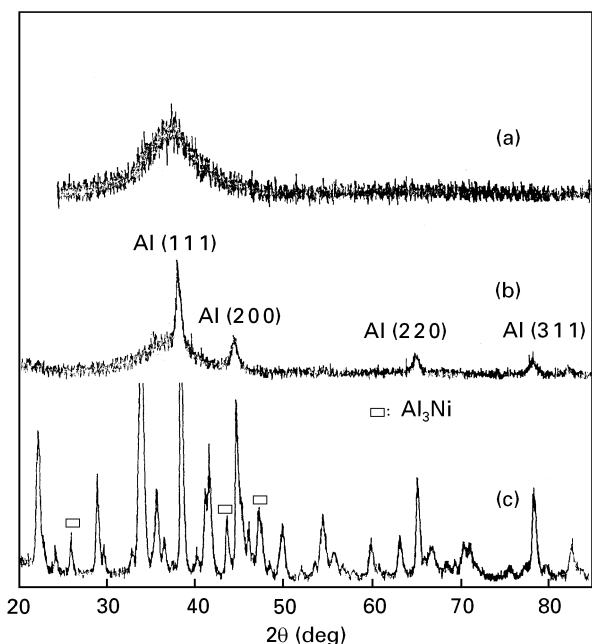


Figure 1 X-ray diffraction patterns of alloys  $\text{Al}_{100-x}\text{RE}_5\text{Ni}_x$ : (a) amorphous phase for  $x = 5, 9, 13, 17, 21$ , (b) amorphous phase + nano fcc-Al for  $x = 5, 9$  heat treated at 453 K for 1 h, (c) completely crystallized state.

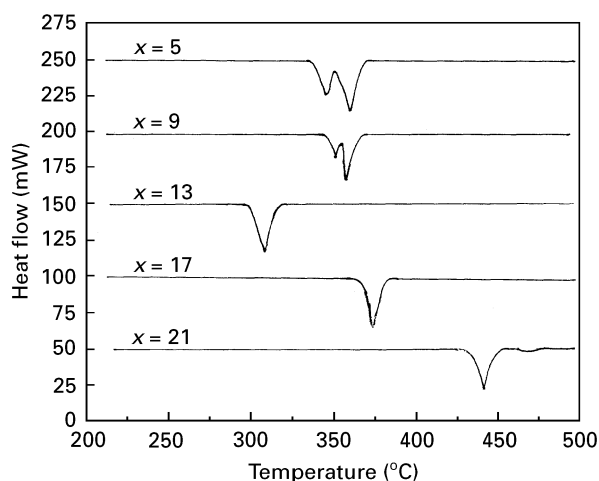
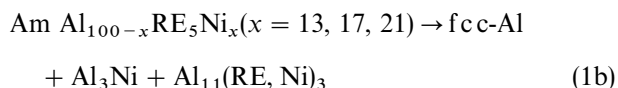


Figure 2 The DSC scanning plots of amorphous  $\text{Al}_{100-x}\text{RE}_5\text{Ni}_x$  alloys at a heating rate of  $20 \text{ K min}^{-1}$ .



The reason for the wider formation range of the ternary Al-RE-Ni amorphous alloys is discussed on the basis of empirical factors for the glass formation of ternary alloys by the liquid quenching technique, namely (1) the different atomic ratios of the constitutive elements, and (2) the stronger interaction between the constitutive atoms is attractive and the mixing enthalpy is relatively large. The size effect and high chemical affinity of rare-earth atoms for nickel and aluminium can better explain the formation ability because it hinders the nickel and aluminium diffusion. The attractive interaction between aluminium and transition metal nickel was taken into consideration in the glass formation of Al-RE-Ni alloys in this paper.

TABLE I The thermal parameters of amorphous  $\text{Al}_{100-x}\text{Ln}_5\text{Ni}_x$  alloys

	$T_x(\text{K})^a$	$T_{p1}(\text{K})^b$	$T_{p2}(\text{K})^c$	$\Delta H(\text{J g}^{-1})^d$
$\text{Al}_{90}\text{RE}_5\text{Ni}_5$	618	620	631	63.5
$\text{Al}_{86}\text{RE}_5\text{Ni}_9$	622	623	629.3	82.6
$\text{Al}_{82}\text{RE}_5\text{Ni}_{13}$	580		581	128.7
$\text{Al}_{78}\text{RE}_5\text{Ni}_{17}$	646		648	104.3
$\text{Al}_{74}\text{RE}_5\text{Ni}_{21}$	714		715	63

<sup>a</sup> $T_x$  the initial crystallized temperature. <sup>b</sup> $T_{p1}$  the temperature of the first exothermic peak of the DSC curves. <sup>c</sup> $T_{p2}$  the temperature of the second exothermic peak. <sup>d</sup> $\Delta H$  the crystallization enthalpy.

We consider that the ordered atomic clusters and disordered atoms may coexist during liquid quenching in the amorphous aluminium-based alloys. There are three kinds of atomic clusters: Al-Al, Al-Ni and Al-RE clusters. The Al-Ni cluster is the structure unit of the intermetallic compound  $\text{Al}_3\text{Ni}$ . The Al-RE cluster is the structure unit of  $\text{Al}_{11}\text{RE}_3$  in amorphous  $\text{Al}_{100-x}\text{RE}_5\text{Ni}_x$  alloys. So fcc-Al is the primary cause of the crystallization process. The stronger interaction in the Al-Ni and Al-RE clusters is attractive, because the crystallization products are intermetallic compounds  $\text{Al}_3\text{Ni}$ , and  $\text{Al}_{11}\text{RE}_3$ .

A large number of alloy systems were found to form metallic glasses when they were rapidly quenched from the liquid state. A group of ductile metallic glasses with aluminium contents up to 90 at % have recently been discovered [7]. Metallic glasses with such a high concentration of the primary element usually cannot be formed by rapid quenching, as most fail to satisfy the atomic-size criterion for glass formation. A number of factors have been proposed as the glass-formation factors. They include the atomic-size ratio, heat of alloy formation and valence electron concentration [8, 9].

Egami and Waseda [10] reported the atomic-size rule for the glass formation of binary alloys. They proposed that, when an element B is alloyed into an element A, there is a close relationship between the minimum concentration of element B,  $C_B$ , and the atomic mismatch. The differential atomic volume ratio was found to be inversely proportional to the minimum solute concentration necessary to form a stable glass phase by rapidly quenching in two-element alloys. The approximate relationship is given by [10]

$$C_B|(V_A - V_B)/V_A| \approx 0.1 \quad (2)$$

where  $C_B$  is the minimum concentration of element B in the element A matrix,  $V_A$  and  $V_B$  are the regular atomic volumes of elements A and B, respectively.

In this investigation, Equation 2 can be extended to ternary alloys by summing the products of the minimum atomic concentration and atomic volume ratio of each solute element, C is the other solute atom in the matrix A

$$S = C_B|(V_A - V_B)/V_A| + C_C|(V_A - V_C)/V_A| \quad (3)$$

TABLE II  $S$  values of amorphous  $\text{Al}_{100-x}\text{RE}_5\text{Ni}_x$  alloys

Alloy	$\text{Al}_{90}\text{RE}_5\text{Ni}_5$	$\text{Al}_{86}\text{RE}_5\text{Ni}_9$	$\text{Al}_{82}\text{RE}_5\text{Ni}_{13}$	$\text{Al}_{78}\text{RE}_5\text{Ni}_{17}$	$\text{Al}_{74}\text{RE}_5\text{Ni}_{21}$
$S$	0.077	0.090	0.104	0.118	0.132

For  $A = \text{Al}$ ,  $B = \text{RE}$  and  $C = \text{Ni}$ , the regular atomic volume is 10.0, 22.0 and  $6.6 \text{ cm}^3 \text{ mol}^{-1}$ . Ohnuma *et al.* [11] successfully described the glass-forming range in the Co–TM–B system (TM = Ti, Zr, Hf, Cr, Mo etc.) using Equation 3;  $S$  is expected to be close to 0.1 [9]. Table II shows the different  $S$  values of amorphous  $\text{Al}_{100-x}\text{RE}_5\text{Ni}_x$  alloys. For  $x = 5$  and 9,  $S$  is less than the expected value 0.1, indicating that the concentrations of nickel and RE are less than those required by this equation. This is mainly due to the small atomic size difference between aluminium and nickel. Aluminium has three valence electrons per atom and high electron density with a high Fermi level. Nickel has eight d-orbital electrons whose Fermi level is lower than that of aluminium. The different Fermi energy may lead to a large amount of transfer of electrons from aluminium to nickel; therefore in a metallic system such a large amount of internal polarization is unstable. So the effective size of nickel will be reduced to increase the Fermi level, while that of aluminium will be increased to balance the flow of charge.

### 3.2. The mechanical properties of amorphous alloys $\text{Al}_{100-x}\text{RE}_5\text{Ni}_x$

The microhardness of amorphous alloys  $\text{Al}_{100-x}\text{RE}_5\text{Ni}_x$  was investigated with a Vicker's hardness tester. The mean of five measurements was used to determine previously the microhardness in each case. For  $x = 5, 9, 13$ , the microhardness increases somewhat with nickel content (Fig. 3), but the microhardness values all equal 2.7 GPa for  $x = 13, 17, 21$ . The marked dependence of microhardness  $H_v$  on nickel content indicates that the bond strength in the aluminium-based glassy structure is determined sensitively by the extent of Al–Ni interaction, or covalency. The enhancement in hardness with increasing nickel content

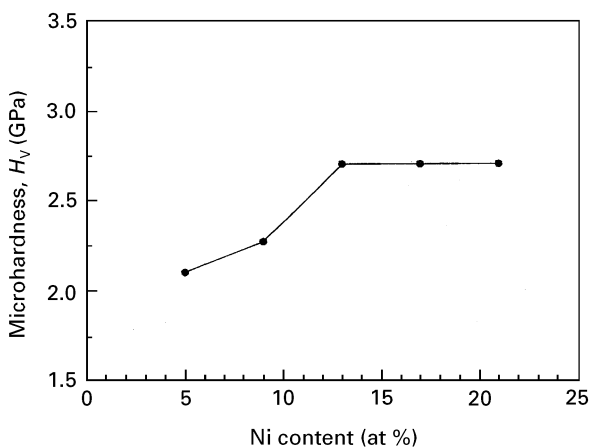


Figure 3 Variations of the microhardness,  $H_v$ , with nickel content of amorphous  $\text{Al}_{100-x}\text{RE}_5\text{Ni}_x$  alloys.

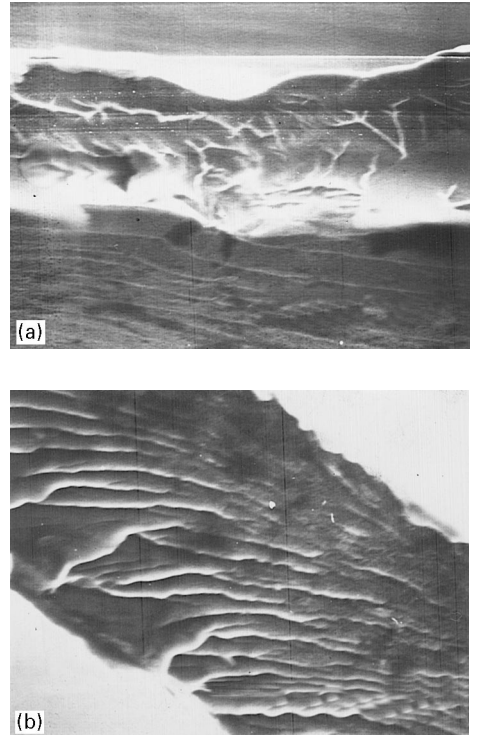


Figure 4 (a) SEM tensile fractograph of amorphous alloy  $\text{Al}_{86}\text{RE}_5\text{Ni}_9$ . (b) SEM tensile fractograph of amorphous alloy  $\text{Al}_{82}\text{RE}_5\text{Ni}_{13}$ .

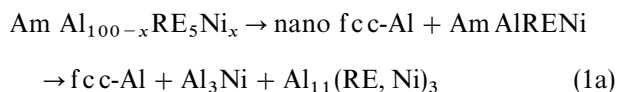
can similarly be explained in terms of an increased influence of Al–Ni covalency. The degree of covalent character in the alloy would be expected to increase gradually as nickel replaces aluminium. This ductile–brittle transition is evidently influenced by the effect of composition and bond rigidity. The amorphous alloys  $\text{Al}_{90}\text{RE}_5\text{Ni}_5$  and  $\text{Al}_{86}\text{RE}_5\text{Ni}_9$  are ductile, the others are brittle. This embrittling effect at higher nickel content is a cause for concern with respect to potential structural applications, because it negates other benefits derived from nickel additions. Fig. 4a shows the SEM tensile fractograph of  $\text{Al}_{90}\text{RE}_5\text{Ni}_5$  amorphous alloys. The fractograph consists of two regions: one is glossy and uncharacteristic, the other shows characteristic vein patterns, similar to those first reported for palladium-based metallic ribbon which had failed in tension [12]. Fig. 4b shows the tensile fractograph of an amorphous alloy  $\text{Al}_{82}\text{RE}_5\text{Ni}_{13}$ , with typical vein patterns of brittle fracture. Additionally, there was evidence for the presence of internal voids.

## 4. Conclusions

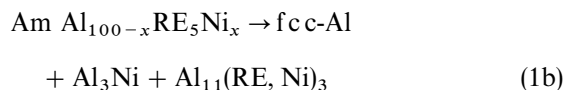
1. The different thermal stabilities and crystallization processes of  $\text{Al}_{100-x}\text{RE}_5\text{Ni}_x$  amorphous alloys were obtained. The final crystallization products are

the same. The crystallization process can be written:

for  $x = 5, 9$



for  $x = 13, 17, 21$



The effective atomic sizes of aluminium and nickel can be changed due to their stronger interaction and different electron structure. The criterion of atomic volume should be modified properly in order to describe the formation mechanism in the amorphous Al-RE-Ni system.

2. Toughness was affected adversely by increasing nickel content. The amorphous alloys were ductile for  $x = 5, 9$ . The others were brittle. The ductility of as-cast aluminium-based amorphous alloys was sensitively dependent on the nickel content. This effect can be explained in terms of the degree of covalency associated with nickel concentrations. The microhardness increased somewhat with increasing nickel content.

## References

1. K. H. J. BUSCHOW, in "Handbook on the physics and chemistry of rare earths", edited by K. A. Gschneidner Jr and L. Eying (Elsevier, Amsterdam, 1984) p. 265.
2. M. HAHIWARA, A. INOUE and T. MASUMOTO, *Metall. Trans.* **13A** (1982) 373.
3. S. HATFA and T. MIGOGUCHI, *Jpn J. Appl. Phys.* **27** (1988) 2078.
4. K. H. J. BUSCHOW, *J. Alloy. Compos.* **193** (1993) 223.
5. A. INOUE, K. OHTERA, K. KITA and T. MASUMOTO, *Jpn J. Appl. Phys.* **27** (1988) L1796.
6. A. INOUE, K. OHTERA, E. TAO and T. MASUMOTO, *ibid.* **27** (1988) L1583.
7. Y. HE, S. J. POON and G. J. SHIFLET, *Science* **241** (1988) 1640.
8. B. C. GIESSEN, in "Proceedings of the 4th International Conference on Rapidly Quenched Metals", Vol. 1, edited by T. Masumoto and K. Suzuki (Japan Inst. Metals, Sendai, 1982) p. 213.
9. S. R. NAGEL and J. TAUC, *Phys. Rev. Lett.* **35** (1975) 380.
10. T. EGAMI and Y. WASEDA, *J. Non-Cryst. Solids* **64** (1984) 113.
11. S. OHNUMA, J. KANEHIRA, K. SHIRAKAWA and T. EGAMI, in "Proceedings of the 4th International Conference on Rapidly Quenched Metals", Vol. 2, edited by T. Masumoto and K. Suzuki (Japan Inst. Metals, Sendai, 1982) p. 1047.
12. F. SPAEPEN, *Acta Metall.* **23** (1975) 615.

*Received 4 December 1995  
and accepted 10 March 1997*